The Astrophysical Journal, 810:141 (10pp), 2015 September 10 doi:10.1088/0004-637X/810/2/141

MODULATION OF GALACTIC ELECTRONS IN THE HELIOSPHERE DURING THE UNUSUAL SOLAR MINIMUM OF 2006–2009: A MODELING APPROACH

M. S. Potgieter[1], E. E. Vos[1], R. Munini[2], M. Boezio[2], and V. Di Felice[3,4]
[1] Centre for Space Research, North-West University, 2520 Potchefstroom, South Africa; Marius.Potgieter@nwu.ac.za.
[2] INFN, Sezione di Trieste, Padriciano 99, I-34012 Trieste, Italy
[3] INFN, Sezione di Roma Tor Vergata, I-00133 Rome, Italy
[4] Agenzia Spaziale Italiana (ASI) Science Data Center, Via del Politecnico snc, I-00133 Rome, Italy
Received 2015 June 23; accepted 2015 July 23; published 2015 September 8

ABSTRACT

The last solar minimum activity period, and the consequent minimum modulation conditions for cosmic rays, was unusual. The highest levels of Galactic protons were recorded at Earth in late 2009 in contrast to expectations. A comprehensive model was used to study the proton modulation for the period from 2006 to 2009 in order to determine what basic processes were responsible for solar modulation during this period and why it differs from proton modulation during previous solar minimum modulation periods. This established model is now applied to studying the solar modulation of electron spectra as observed for 80 MeV–30 GeV by the *PAMELA* space detector from mid-2006 to the end of 2009. Over this period the heliospheric magnetic field had decreased significantly until the end of 2009 while the waviness of the heliospheric current sheet decreased moderately and the observed electron spectra increased by a factor of ∼1.5 at 1.0 GeV to ∼3.5 at 100 MeV. In order to reproduce the modulation evident from seven consecutive semesters, the diffusion coefficients had to increase moderately while maintaining the basic rigidity dependence. It is confirmed that the main diffusion coefficients are independent of rigidity below ∼0.5 GV, while the drift coefficient had to be reduced below this value. The 2006–2009 solar minimum epoch indeed was different than previously observed minima, at least since the beginning of the space exploration era. This period could be called "diffusion-dominated" as was also found for the modulation of protons.

Key words: cosmic rays – stars: activity – Sun: heliosphere

1. INTRODUCTION

The modulation conditions for Galactic cosmic rays (CRs) in the heliosphere were unusual for the recent solar minimum activity period up to the end of 2009. The new activity cycle did not begin in early 2008, but instead minimum modulation conditions continued until the end of 2009; this period was characterized by a much weaker heliospheric magnetic field (HMF) compared with those of previous cycles. The tilt angle α of the wavy heliospheric current sheet (HCS), on the other hand, had not decreased as rapidly (relatively speaking) as the magnitude of the HMF at Earth during this period, but eventually also reached a minimum value at the end of 2009. During this prolonged solar minimum period, Galactic protons also responded differently compared to previous solar minima as illustrated by Potgieter et al. (2014). These authors utilized *PAMELA* proton observations (Adriani et al. 2013) and a comprehensive solar modulation model including gradient, curvature, and HCS drifts to study the period from mid-2006 to the end of 2009 in detail. Here, we continue this study but now focus on the electron observations made by *PAMELA* over the mentioned period (Adriani et al. 2015).

First, we note that drift models predict that during $A < 0$ polarity cycles of the HMF, all positively charged CRs drift toward Earth mostly but not exclusively along the wavy HCS, while electrons drift mainly over the heliospheric polar regions. During these cycles, the HCS plays a less evident but still important role for negatively charged particles. If this type of particle drift was always dominant during solar minimum activity periods in the heliosphere, then we would predict that for identical modulation conditions, proton spectra for $A < 0$ minimum cycles should be lower than spectra during $A > 0$ cycles at kinetic energies $E < \sim 1$ GeV (see, e.g., Potgieter 2014a). However, the proton spectra observed by the *PAMELA* mission before 2010, as reported by Adriani et al. (2013), showed that this did not happen in 2009. In fact, the highest proton spectra were measured then; see the compilation by Strauss & Potgieter (2014a). Simulations of this period with a comprehensive numerical model by Potgieter et al. (2014) explained why it happened. The reason is that during these ideal minimum modulation conditions the spatial gradients in the CR intensity became small as a result of less overall diffusion, which caused drift effects to be less evident despite the CR particles actually experiencing large drift velocities. For a comprehensive report of the solar modulation of CRs, see the review by Potgieter (2013).

Following the reasoning given above, the same modeling approach is tested here for CR electrons. As mentioned, during $A < 0$ cycles electrons drift toward the Earth mostly but not exclusively through the polar regions of the heliosphere, eluding the impact of the wavy HCS on CR modulation. Together with the HMF magnitude, the waviness of the HCS, as represented by its tilt angle (Hoeksema 1991), is considered an excellent proxy for solar activity when it comes to the solar modulation of charged particles. This causes charge-sign dependent modulation, implying that CR electrons should experience less modulation over the same period under the same solar activity conditions, such as from 2006 to 2009. In order to test this prediction, electron spectra of a high quality are required in the energy range where CR drifts are predicted to give significant effects, typically between ∼50 MeV and ∼5 GeV, with a maximum effect (measured by the difference between $A > 0$ and $A < 0$ spectra) between 100 and 300 MeV (e.g., Ferreira 2005). For a discussion of these specific drift effects, see the review by Potgieter (2014a). Fortunately, the

PAMELA mission can provide such spectra, measured by the same instrument over the same period. Final electron spectra, for seven periods of six-month averages, referred to as seven semesters, between mid-2006 and the end of 2009 are reported by Adriani et al. (2015). The modulation of these spectra is studied here by using a comprehensive three-dimensional (3D) numerical model, similar to the one used for studying the *PAMELA* proton spectra for the same period (Potgieter et al. 2014). The purpose is to simulate these observed electron spectra using the exact same modulation approach as for the protons, but with the drift velocity directions changed. This will verify the general conclusions made about the modulation processes during this period as found for protons.

This work is therefore focused on electron modulation and will be followed by a paper on charge-sign dependent modulation directly comparing the observed electron and proton spectra with the corresponding simulations for 2006–2009. As soon as the observed positron spectra from *PAMELA* are finalized, a comparison will be made between the charge-sign dependence that follows from electron to proton ratios and from electron to positron ratios for the mentioned period.

2. *PAMELA* ELECTRON OBSERVATIONS FROM 2006 TO 2009

PAMELA is a satellite-borne experiment designed for CR antimatter studies. The instrument has been flying on board the Russian *Resurs-DK1* satellite since 2006 June, following a semi-polar near-Earth orbit (see, e.g., Boezio et al. 2009; Adriani et al. 2011). Adriani et al. (2013) presented proton observations down to 400 MV from 2006 July until 2009 December which made a significant contribution to the understanding of solar modulation below ∼30 GeV (see Strauss & Potgieter 2014b for where solar modulation commences in terms of energy). This was followed by finalized electron spectra as reported by Adriani et al. (2015). For the experimental reasons that they discussed, the electron spectra are not reported for every Carrington rotation of the Sun as was done for protons but instead as seven six-month (semester) averages. Progress reports with preliminary electron spectra were made from time to time; see, e.g., Di Felice (2010), Munini et al. (2013), and Vos et al. (2013). Review papers on *PAMELA* electron observations, e.g., by Mocchiutti et al. (2011), Menn et al. (2013), and references therein, were mainly focused on astrophysical aspects with electron spectra reported above 1 GeV.

In Figure 1 the observed electron spectra are shown; they were obtained by averaging over six-month periods to give seven semesters, starting from 2006 July and ending in 2009 December. Because a Forbush-type decrease was observed in 2006 December, it was removed from that semester interval. All these spectra were thus observed during an $A < 0$ magnetic polarity cycle with emphasis on the energy range from 80 MeV and up to 30 GeV where solar modulation is assumed to be negligible. In 2010 January, solar activity had picked up significantly so that the CR intensity started to decrease and observations beyond 2009 December are therefore excluded. Apart from the evident increasing modulation with decreasing energy, the other main features are: the spectra exhibit maximum values between ∼500 and ∼800 MeV and these maxima shift gradually to lower energies during this period. At around 100 MeV, the spectra show minima that shift gradually

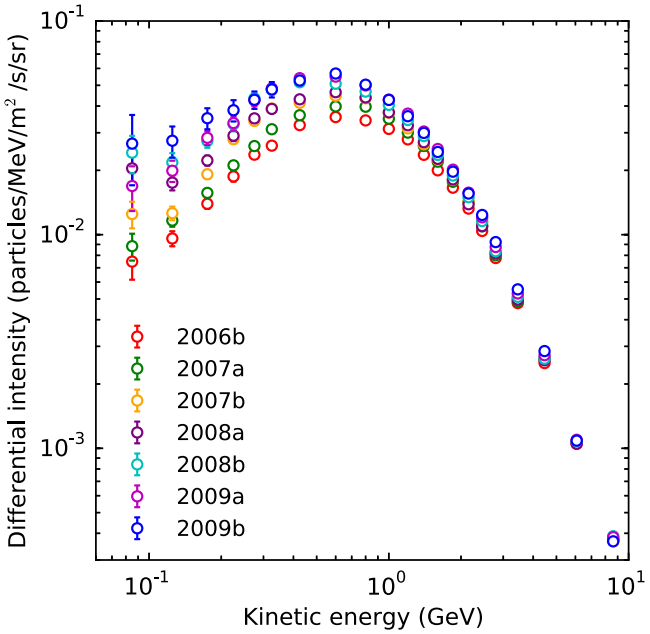

Figure 1. Solar modulation of electron energy spectra observed by the *PAMELA* mission, shown here as six-month averages for seven semesters, starting from 2006b, indicating the second semester of 2006 (July–December), up to 2009b as the second semester of 2009. Adapted from Adriani et al. (2015).

to higher energies so that the shape of the spectra changes in particular at the lowest energies where the spectral form gets progressively flatter around 100 MeV to be clearly flat in 2009a and 2009b. These features will be investigated with the numerical model.

In order to emphasize how decreasing solar modulation conditions allowed Galactic electrons to increase at Earth over this 3.5 year period, especially at $E < \sim 10$ GeV, the spectra in Figure 1 are used to calculate and plot the intensity ratios as a function of E with respect to the second semester of 2006, again indicated as 2006b. This is shown in Figure 2. Together with Figure 1, this illustrates how the electron spectra unfolded with energy and with time from mid-2006 to the end of 2009.

These seven spectra were selected to be studied and to be reproduced with the modulation model discussed below. For this purpose, the relevant modulation conditions, as a prerequisite for applying the modulation model, have been studied and are given next.

In Figure 3 the relevant heliospheric modulation conditions based on a selection of observations are illustrated from the year 2000 to solar minimum activity conditions before and in 2009 up to 2012. The top panel shows the sunspot number (http://sidc.oma.be/), which had already evidently become quite low in 2007, remaining very low until it began to increase in 2009 to start a new sunspot cycle. The second panel gives the count rate of the Hermanus Neutron Monitor (NM), normalized to 100% in 1987 March, as an indication of how CRs at relatively high rigidity responded to the decrease in solar activity. This NM data show a steep increase from 2006 to 2007 with a plateau in 2008 and a clear maximum from early 2009 until late 2009. By 2010 January these high-rigidity CRs had begun to decrease. The third panel shows the HCS tilt angle for the same period which is, from a modulation modeling point of view, an excellent proxy for solar activity. Qualitatively, the message is the same but the tilt angle α did

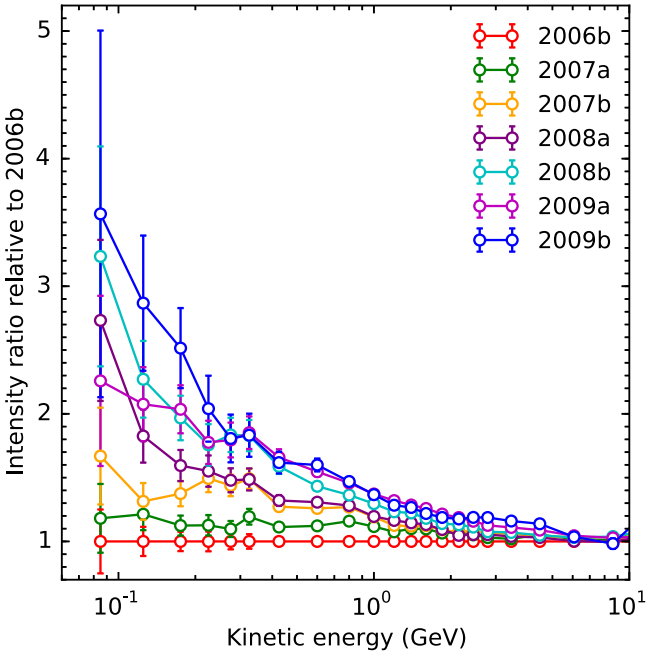

Figure 2. Using the observed spectra in Figure 1, the flux ratios for each consecutive semester are shown as a function of kinetic energy with respect to the second semester of 2006 (2006b) up to second semester of 2009 (2009b). The lines connecting the data points are to guide the eye in order to see how the spectra unfolded and got progressively softer.

not decrease as quickly as in previous solar minimum periods, remaining at relatively high values from 2006 to 2008. Only in 2009 did α drop to values less than 10°, which is considered prime solar minimum conditions. It began to increase from the last days of 2009 December and then significantly from early in 2010 January, reaching 60° in 2011. This type of fast increase also happened after previous solar minima. In the fourth panel the monthly and daily HMF averages observed at Earth by the *Advanced Composition Explorer* (*ACE*) are shown as a function of time. In contrast to previous solar minima, the averaged HMF value dropped to ~3.9 nT for an extended period of time and sporadically dropped below even this value as was also pointed out by Cliver et al. (2011). This is considered unusual; see also the review by Kóta (2013).

The changes in α and HMF values are most relevant for modeling and are emphasized in Figures 4(a) and (b), respectively, by plotting them on a larger scale for the period 2006–2010. In order to produce electron spectra for a specific period such as the second semester of 2006b, with the 3D model described below, the averaged α and HMF values are required for the preceding 16 months (as a maximum) to 10 months (as a minimum) as input parameters for the model. This procedure is required because CRs respond to modulation conditions between the modulation boundary, assumed to be the heliopause (HP), and the point of observation, in this case at the Earth. The averaged α between Earth and the modulation boundary must be estimated based on what had been observed over at least 12 months before the observational time of the particular CR spectrum. We proceed to calculating the average tilt angle (which always moves outward with the slowest solar wind speed) and average HMF values (which move outward in this 3D approach as the average of the slowest and fastest solar wind speeds) as shown in Figures 4(a) and (b) and also listed in the first two rows of Table 1 for 2006b, 2007a, 2007b, 2008a, 2008b, 2009a, and 2009b, respectively. These averages are used as observationally motivated input to our model, with the diffusion coefficients and drift coefficient (being theoretically motivated) recalculated every time for the seven selected time periods. These coefficients and how they relate to the HMF values and particularly their rigidity dependence are discussed in Section 4.

3. THE VERY LOCAL INTERSTELLAR SPECTRUM FOR ELECTRONS AND THE HELIOSPHERIC MODULATION BOUNDARY

A Galactic electron spectrum, or more specifically a very local interstellar spectrum (LIS), has to be specified in modulation models as an initial condition to be used as the input spectrum which is then modulated from a given heliospheric boundary up to Earth. The value of such a very LIS (sometimes also referred to as a heliopause spectrum, HPS) below a few GeV, where modulation effects are considered to be important, has always been rather contentious; see the discussion by Potgieter & Nndanganeni (2013a). Fortunately, this situation improved significantly when *Voyager 1* crossed the HP at 121.7 AU in 2012 August and has since been exploring the very local interstellar medium (Gurnett et al. 2013). A new very LIS has been constructed subsequently for this study, incorporating the *Voyager 1* observations between 5 and 50 MeV (Stone et al. 2013) and the *PAMELA* observations above 30 GeV; see also Potgieter (2014b) for an overview. A preliminary report on this effort was made by Vos et al. (2013) who pointed out that the *PAMELA* electron spectra contain an interesting spectral index change between ~5 and ~15 GeV which had to be incorporated in the construction of this very LIS. The significance of this feature will be addressed in a separate publication. Here, it suffices to say that if this spectral change is ignored, the LIS based on high energies, $E > 30$ GeV, or as predicted by the well-known GALPROP code (e.g., Strong et al. 2011), falls below the observed electron flux at the Earth in this energy range which is totally unacceptable from a modulation point of view. Fortunately, including this feature, referred to as $J_{\rm bump}$, does not at all change the qualitative conclusions of the work reported here, but it does affect the values of the diffusion coefficients that are needed in the model to reproduce the observed spectra in this particular energy range. However, as will become evident, the total modulation at these energies is less than at lower energies with $E < 500$ MeV.

The very LIS for electrons that we constructed is given in terms of differential intensity in units of particles $\rm m^{-2}\,s^{-1}\,sr^{-1}\,MeV^{-1}$ as

$$J_{\rm LIS} = (0.21)\left(\frac{E^{-1.35}}{\beta^2}\right)\left[\frac{E^{1.65}+0.6920}{1.6920}\right]^{-1.1515} + J_{\rm bump} \quad (1)$$

with E the kinetic energy in GeV, with

$$J_{\rm bump} = 1.73\,\exp\left[4.19-5.40\log(E) - 8.9\left(E^{-0.64}\right)\right], \quad (2)$$

and with $\beta = v/c$, the ratio of the electron's speed to the speed of light. This LIS will be shown together with the modeled spectra in figures to follow.

One additional relevant remark in this context is that Scherer et al. (2011) argued that the solar modulation of

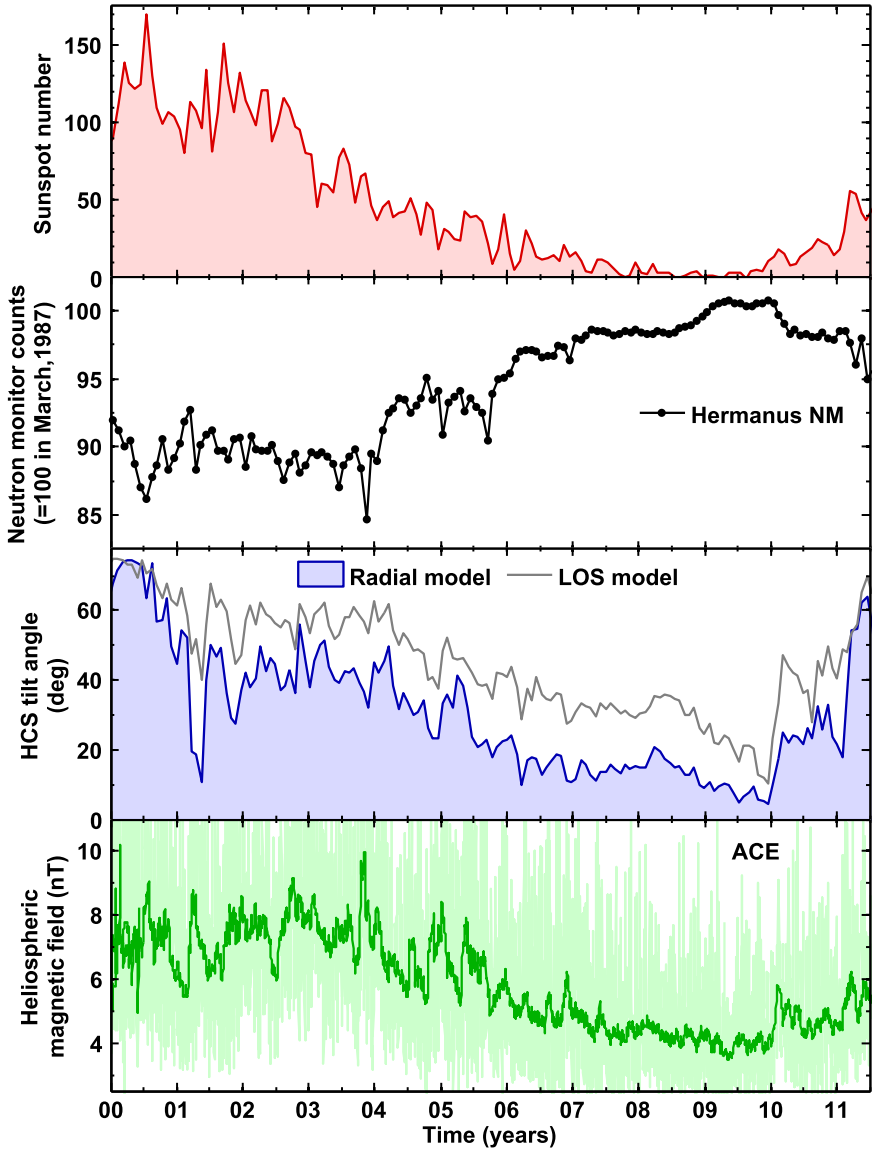

Figure 3. Heliospheric modulation conditions from the year 2000 (indicated by 00) to solar minimum activity in 2009 and up to 2012. The top panel shows the observed sunspot numbers (http://sidc.oma.be/) and the second panel gives the count rate of the Hermanus neutron monitor (NM) normalized to 100% in 1987 March (http://www.nwu.ac.za/content/neutron-monitor-data). The third panel shows the HCS tilt angle based on two approaches (radial model and LOS model; see http://wso.stanford.edu/). The fourth panel gives the monthly (dark green line) and daily (light green line) HMF averages observed at Earth by *ACE* (http://nssdc.gsfc.nasa.gov/).

Galactic CRs might start well beyond the HP which has been considered by most as the true CR modulation boundary. The effect is small; a reduction of ∼25% at $E = 100$ MeV was computed over the entire outer heliosheath for protons by Strauss et al. (2013). Since this controversial issue cannot yet been settled (*Voyager 1* is presently only at ∼132 AU from the Sun), we continue to assume the HP as the boundary where the modulation of CRs essentially commences, which is assumed to be at 122 AU for this work. The very LIS is then specified at the HP position.

4. THEORY, NUMERICAL MODEL, AND MODULATION PARAMETERS

A full 3D model is used to compute the differential intensity of 10 MeV–50 GeV CR electrons at Earth. It is based on the numerical solution of the well-known heliospheric transport equation (TPE; Parker 1965)

$$\frac{\partial f}{\partial t} = -\left(\boldsymbol{V} + \langle \boldsymbol{v}_{\rm D} \rangle\right).\nabla f + \nabla.\left(\mathbf{K}_{\rm s}.\nabla f\right) + \frac{1}{3}(\nabla.\boldsymbol{V})\frac{\partial f}{\partial \ln P}, \quad (3)$$

where $f(\boldsymbol{r}, P, t)$ is the CR distribution function, P is rigidity, t is time, and $\boldsymbol{r}$ is the vector position in 3D, with the usual three coordinates r, θ, and φ specified in a heliocentric spherical coordinate system where the equatorial plane is at a polar angle of $\theta = 90°$. Since we address a solar minimum modulation period with gradual changes in the modulating parameters, it is assumed that $\partial f/\partial t = 0$. Terms on the right-hand side respectively represent convection, with $\boldsymbol{V}$ the solar wind velocity; averaged particle drift velocity $\langle \boldsymbol{v}_{\rm D} \rangle$ caused by gradients, curvatures, and HCS drifts in the global HMF; diffusion, with $\mathbf{K}_{\rm s}$ the symmetry diffusion tensor and then

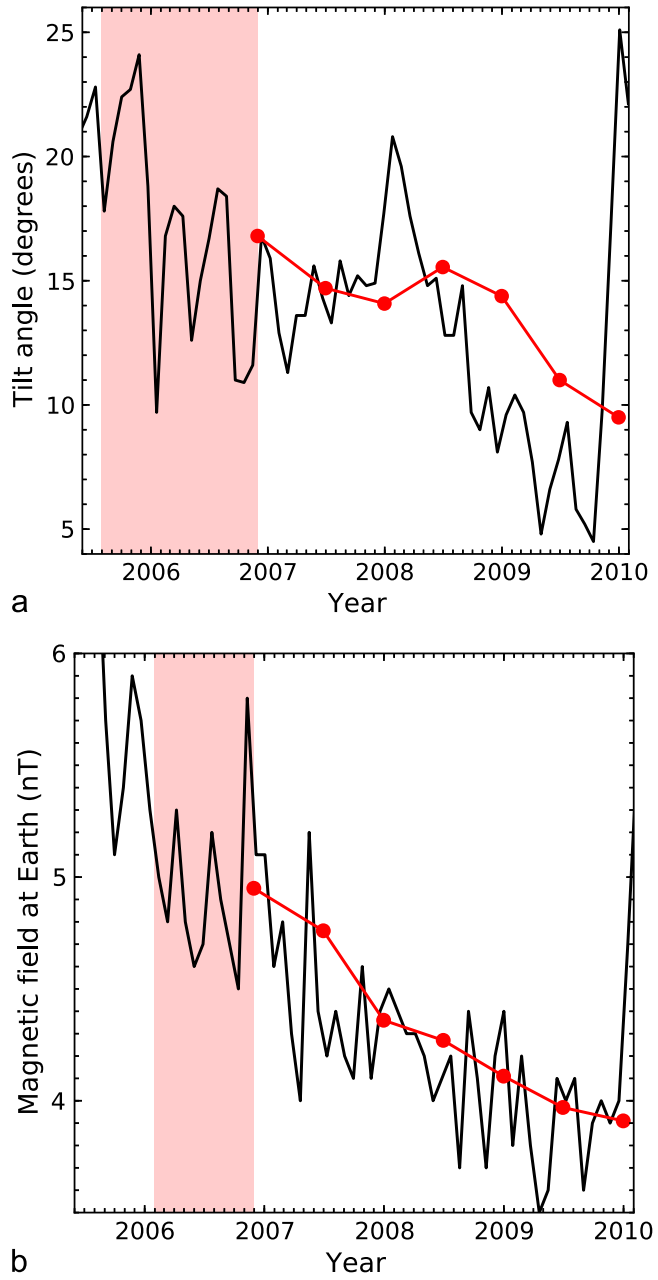

Figure 4. (a) Observational HCS tilt angles at Earth (black curve) from Figure 3 and how they were averaged for the selected seven semesters for the modeling study (red curve). The first red point is the average value for the preceding 16 months as indicated by the colored band. The same was done for all the other points up to the beginning of 2010. The red points are therefore the averaged HCS tilt angle values used as input for the modeling runs to compute the seven averaged electron spectra at Earth. (b) The observational HMF values at Earth (black curve) from Figure 3 and how they were averaged for the CR modeling study (red curve). The first red point is the average value for the preceding 10 months as indicated by the colored band. The same was done for all the other points up to the beginning of 2010. The red points are therefore the HMF values used as input for the CR modeling runs to compute the seven averaged electron spectra.

adiabatic energy changes, with $(\nabla .\, \boldsymbol{V}) > 0$ giving adiabatic energy losses except inside the heliosheath where it is assumed that $(\nabla .\, \boldsymbol{V}) = 0$. Adiabatic energy change is one of the four major modulation mechanisms and is crucially important for Galactic CR modulation in the inner heliosphere but far less dominant for electrons than for protons (see the illustrations by Strauss et al. 2011).

Following Potgieter et al. (2014), the TPE is solved in a heliocentric spherical coordinate system so that the geometry of the HMF comes into play through the HMF spiral angle ψ to give the nine elements of the full tensor as

$$\begin{aligned} K_{rr} &= K_{\parallel}\cos^2\psi + K_{\perp r}\sin^2\psi, \\ K_{\perp\theta} &= K_{\theta\theta}, \\ K_{\phi\phi} &= K_{\perp r}\cos^2\psi + K_{\parallel}\sin^2\psi, \\ K_{\phi r} &= \left(K_{\perp r} - K_{\parallel}\right)\cos\psi\sin\psi = K_{r\phi}, \\ K_{\theta r} &= K_d\sin\psi = -K_{r\theta}, \\ K_{\theta\phi} &= K_d\cos\psi = -K_{\phi\theta}, \end{aligned} \tag{4}$$

with K_{rr}, $K_{r\phi}$, $K_{\theta\theta}$, $K_{\phi r}$, $K_{\phi\phi}$ describing the diffusion processes and $K_{r\theta}$, $K_{\theta r}$, $K_{\phi\theta}$, $K_{\theta\phi}$ describing particle drifts. Here, K_{rr} is the effective radial diffusion coefficient and thus a combination of the parallel diffusion coefficient $K_{\parallel}$ and the radial perpendicular diffusion coefficient $K_{\perp r}$; $K_{\theta\theta} = K_{\perp\theta}$ is the effective diffusion coefficient perpendicular to the HMF in the polar direction, whereas $K_{\phi\phi}$ describes the effective diffusion in the azimuthal direction, and so on. Inspection shows that the five diffusion coefficients are determined by what is assumed for parallel and perpendicular diffusion, and all of them depend on the geometry of the assumed HMF. For instance, beyond ~20 AU in the equatorial plane the HMF spiral $\psi \rightarrow 90°$, so that K_{rr} is dominated by $K_{\perp r}$ but by $K_{\parallel}$ in the polar regions of the heliosphere, whereas $K_{\phi\phi}$ is dominated by $K_{\parallel}$. This is true only if the HMF is Parkerian in its geometry. The four drift coefficients are given in the last two rows of Equation (4). These nine tensor elements will become significantly more complicated if the HMF geometry contains a latitudinal component which is not considered for this study (see, e.g., Effenberger et al. 2012).

Following Potgieter et al. (2014), the magnitude of the solar wind velocity during solar minimum activity periods up to the HP at 122 AU is given by

$$\begin{aligned} V(r,\,\theta) = V_0 &\left\{1 - \exp\left[13.33\left(\frac{r_{\rm sun} - r}{r_0}\right)\right]\right\} \\ &\times \left\{1.475 \mp 0.4\tanh\left[6.8\left(\theta - \frac{\pi}{2} \pm \theta_T\right)\right]\right\} \\ &\left[\frac{(s+1)}{2s} - \frac{(s-1)}{2s}\tanh\left(\frac{r - r_{\rm TS}}{L}\right)\right], \end{aligned} \tag{5}$$

where $V_0 = 400\,{\rm km\,s^{-1}}$, $r_{\rm sun} = 0.005$ AU, $r_0 = 1$ AU, $s = 2.5$, and $L = 1.2$ AU. The top and bottom signs correspond to the northern $(0 \leqslant \theta \geqslant \pi/2)$ and southern hemispheres $(\pi/2 \leqslant \theta \geqslant \pi)$ of the heliosphere, with $\theta_T = \alpha + 15\pi/180$. This determines at which polar angle the solar wind speed changes from a slow to a fast region. Here, L is the shock scale length and s is the compression ratio of the termination shock (TS) which changed position from 88 AU in 2006 to 86 AU in 2007, 84 AU in 2008, and 80 AU in 2009 in this study. The re-acceleration effects of the TS are neglected for the CRs considered here. However, the modulation effect of the heliosheath, which is at least 34 AU wide in our model, has

Table 1
Summary of Input and Modulation Parameters Used to Compute the Seven Semester Averages for Electron Spectra That Agree with the *PAMELA* Observations

Parameter	2006b	2007a	2007b	2008a	2008b	2009a	2009b
α(degrees)	16.80	14.70	14.08	15.55	14.38	11.00	9.50
B at Earth (nT)	4.95	4.76	4.36	4.27	4.11	3.97	3.91
$\lambda_{\parallel}$ (AU)[a] $\times 10^{-1}$	1.01	1.07	1.11	1.18	1.25	1.27	1.35
$\lambda_{\perp r}$ (AU)[a] $\times 10^{-3}$	2.85	3.01	3.19	3.32	3.51	3.59	3.78
a	0.0	0.0	0.0	0.0	0.0	0.0	0.0
b_1	1.55	1.55	1.55	1.55	1.55	1.55	1.55
b_2	1.24	1.24	1.24	1.24	1.24	1.24	1.24
c	3.5	3.5	3.5	3.5	3.5	3.5	3.5
P_k (GV)	0.33	0.33	0.33	0.34	0.34	0.34	0.34

Note. See Equations (9)–(11) and (13).
[a] At Earth at 100 MeV.

been incorporated self-consistently through the expressions for the diffusion coefficients (when V drops at the TS, the HMF magnitude increases and thus changes the diffusion coefficients accordingly by the factor s). Beyond the TS, the solar wind profile is assumed to change so that $(\nabla .\, \boldsymbol{V}) = 0$ in Equation (3).

The usual expression for the magnitude of a Parkerian type of HMF is

$$B_{\rm Parker} = B_n \left(\frac{r_0}{r}\right)^2 \sqrt{1 + (\tan\psi)^2} \tag{6}$$

with

$$\tan\psi = \Omega \frac{(r - r_{\odot})}{V} \sin\theta. \tag{7}$$

Here, B_n is the value to which the HMF magnitude is normalized, in this case the value at the Earth; Ω is the rotation speed of the Sun, $r_{\odot} = r_{\rm sun}$ in AU, and V is the solar wind speed as given by Equation (5). This HMF magnitude is modified according to Smith & Bieber (1991), using instead of Equation (7) the following:

$$\tan\psi = \frac{\Omega\left(r - 20r_{\odot}\right)\sin\theta}{V\left(r,\,\theta\right)} - \frac{rV\left(20r_{\odot},\,\theta\right)}{20r_{\odot}V\left(r,\,\theta\right)}\left(\frac{B_T\left(20r_{\odot}\right)}{B_R\left(20r_{\odot}\right)}\right), \tag{8}$$

with the ratio $B_T/B_R = -0.15$. This approach keeps the basic Parkerian geometry but modifies its magnitude progressively toward the poles of the heliosphere. This gives a more realistic modification, based on sound physical arguments, than used before; see the general discussion of the relevance of this modification by Potgieter (2013) and also the recent study by Raath et al. (2015).

A general expression for the diffusion coefficient parallel to the average background HMF is given by

$$K_{\parallel} = \left(K_{\parallel}\right)_0 \beta \left(\frac{B_0}{B}\right)\left(\frac{P}{P_0}\right)^a \left[\frac{\left(\frac{P}{P_0}\right)^c + \left(\frac{P_k}{P_0}\right)^c}{1 + \left(\frac{P_k}{P_0}\right)^c}\right]^{\frac{(b_1 - a)}{c}}, \tag{9}$$

with β as before. Here, $(K_{\parallel})_0$ is a constant in units of $10^{22}\,{\rm cm^2\,s^{-1}}$, with the rest of the equation written to be dimensionless with $P_0 = 1$ GV and B the HMF magnitude as modified above and $B_0 = 1$ nT (so that the units remain ${\rm cm^2\,s^{-1}}$). The constants a, b, and c are given in Table 1; a is a power index that can change with time if required, but here for electrons $a = 0.0$, whereas $b = 1.55$. Together they determe the slope of the rigidity dependence respectively above and below a rigidity with the value P_k,; $c = 3.5$ determines the smoothness of the transition. This means that the rigidity dependence of $K_{\parallel}$ basically has a power-law shape at high rigidities but is independent of rigidity at lower energies, as will be illustrated later (in Figure 7) after the computed spectra are displayed. This assumption is in line with the basic predictions of turbulence theory for low-energy electrons; see, e.g., Teufel & Schlickeiser (2002) and Shalchi (2009).

Perpendicular diffusion in the radial direction is assumed to scale spatially similar to Equation (9) but with a different rigidity dependence at higher rigidities; again with $a = 0.0$ so that

$$K_{\perp r} = 0.02\left(K_{\parallel}\right)_0 \beta \left(\frac{B_0}{B}\right)\left[\frac{\left(\frac{P}{P_0}\right)^c + \left(\frac{P_k}{P_0}\right)^c}{1 + \left(\frac{P_k}{P_0}\right)^c}\right]^{\left(\frac{b_2}{c}\right)}, \tag{10}$$

with $b_2 \neq b_1$. This rigidity dependence is in line with what essentially was proposed by Burger et al. (2000) based on turbulence arguments and will be illustrated below.

The perpendicular diffusion coefficient in the polar direction is assumed to be given by

$$K_{\perp\theta} = K_{\perp r} f_{\perp\theta} \tag{11}$$

with $f_{\perp\theta} = AA^{+} \mp AA^{-} \tanh[8(\theta_A - 90^{\circ} \pm \theta_F)]$. Here, $AA^{\pm} = (d \pm 1)/2$, $\theta_F = 35^{\circ}$, $\theta_A = \theta$ for $\theta \leqslant 90^{\circ}$ but $\theta_A = 180^{\circ} - \theta$ with $\theta \geqslant 90^{\circ}$ and $d = 1.2$. This means that $K_{\theta\theta} = K_{\perp\theta}$ is enhanced toward the poles by a factor d with respect to the value of $K_{\parallel}$ in the equatorial regions of the heliosphere (as also applied and motivated by Potgieter 2000; Ferreira et al. 2003; Moeketsi et al. 2005; Ngobeni & Potgieter 2011; Nkosi et al. 2011). This polar enhancement is less than used before because the background HMF is now modified according to the approach of Smith & Bieber (1991) as discussed above.

The pitch angle averaged guiding center drift velocity for a near isotropic CR distribution is given by $\langle \boldsymbol{v}_{\rm D} \rangle = \nabla \times (K_A \boldsymbol{e}_{\rm B})$, with $\boldsymbol{e}_{\rm B} = \boldsymbol{B}/B$. Under the assumption of weak scattering, the drift coefficient is straightforwardly given as

$$\left(K_A\right)_{\rm ws} = \left(K_A\right)_0 \frac{\beta P}{3B} \tag{12}$$

where is $(K_A)_0$ dimensionless. In this case $(K_A)_0 = 1.0$ describes full gradient and curvature drifts, known as "weak scattering" drifts, and this is theoretically the largest it can be at all rigidities. A deviation from this weak scattering form, given by

$$K_A = \left(K_A\right)_0 \frac{\beta P}{3B}\left(\frac{(P)^2}{1 + (P)^2}\right), \tag{13}$$

is used. This means that from below ~1 GV particle drifts are progressively reduced with respect to the weak scattering case, as will be illustrated below. This is specifically required to explain the small latitudinal gradients at low rigidities observed by *Ulysses* (e.g., Heber & Potgieter 2006; De Simone et al. 2011).

The three drift velocity components in terms of $K_{r\theta}$, $K_{\theta r}$, $K_{\phi\theta}$, $K_{\theta\phi}$ are

$$\begin{aligned}
\langle \boldsymbol{v}_{\rm D} \rangle_r &= -\frac{A}{r \sin\theta}\frac{\partial}{\partial\theta}\left(\sin\theta K_{\theta r}\right), \\
\langle \boldsymbol{v}_{\rm D} \rangle_\theta &= -\frac{A}{r}\left[\frac{1}{\sin\theta}\frac{\partial}{\partial\phi}\left(K_{\phi\theta}\right) + \frac{\partial}{\partial r}\left(rK_{r\theta}\right)\right], \\
\langle \boldsymbol{v}_{\rm D} \rangle_\phi &= -\frac{A}{r}\frac{\partial}{\partial\theta}\left(K_{\theta\phi}\right),
\end{aligned} \tag{14}$$

with $A = \pm 1$; when this value is positive (negative), an $A > 0$ ($A < 0$) polarity cycle is described. For the period studied here, the polarity cycle is indicated by $A < 0$, as was also the case for the time around the solar minimum modulation of 1965 and 1987. For a discussion of the effects of different assumptions of heliospheric turbulence on electron modulation, see Potgieter (1996).

Graphical illustrations of the diffusion coefficients and the drift coefficient as a function of rigidity will be shown below, together with the computed spectra.

5. MODELING RESULTS

To solve the TPE as applicable to the seven semesters (2006b, 2007a, 2007b, 2008a, 2008b, 2009a, and 2009b), the calculated α and observed HMF magnitude at Earth were averaged as discussed above and shown in Figures 4(a), (b). In our modeling approach, this produces the averaged modulation conditions in the global heliosphere for the time period when the electron spectrum for a given semester was observed at Earth.

In Figure 5(a) the *PAMELA* electron spectra from Figure 1 are overlaid by the corresponding computed spectra. During this time α changed from an averaged value of ~16°.8 to ~9°.5, with an accompanying change in the averaged HMF at Earth from $B \sim 4.95$ to ~3.91 nT. Although these changes seem relatively small, they have significant modulation effects because B is directly changing the value of the three diffusion coefficients and the drift coefficient. These results serve to illustrate that the model can reproduce the observed electron spectra for the selected seven semesters when the modulating effects of the various parameters as described above are combined.

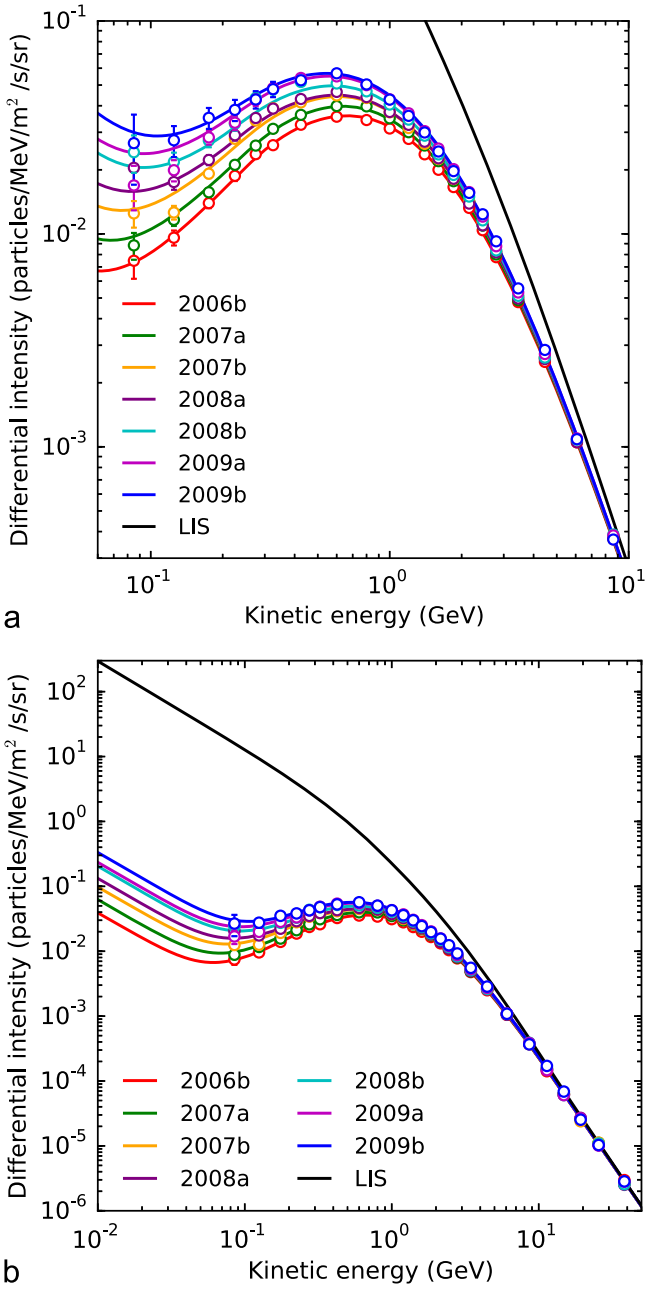

Figure 5. (a) Observed seven electron spectra (colored data points) from Figure 1 overlaid by the corresponding computed spectra (colored solid lines) based on the modulation parameters described in the text and summarized in Table 1. The LIS (Equation (1)) is specified at 122 AU where the HP is located. (b) Similar to Figure 5(a) but now with the computed spectra shown to 10 MeV with respect to the very LIS specified at 122 AU at the HP.

The main features exhibited by the observed spectra are reproduced by the model. They are: (1) the gradual shift in the maximum intensity values between ~500 and ~800 MeV to lower energies from 2006 to 2009 (it follows from the modeling that this occurs because of the changing interplay between drifts and diffusion with decreasing energy) and (2) the gradual shift of the minimum intensity values around 100 MeV to higher energies and the accompanying flattening of the spectra; this occurs as drifts phase out with decreasing

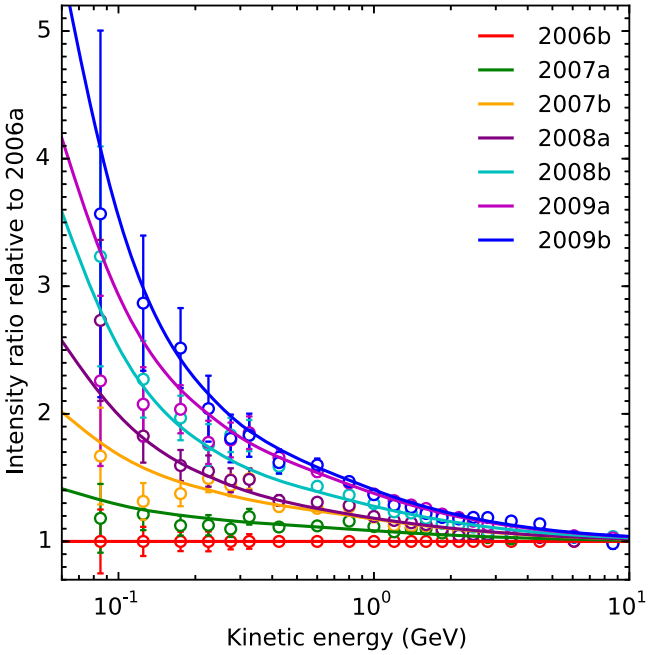

Figure 6. Flux ratios (colored data points with errors bars) with respect to the observed 2006b spectrum, as shown in Figure 2, in comparison with the corresponding ratios (colored solid lines) using the computed spectra in Figure 5(a).

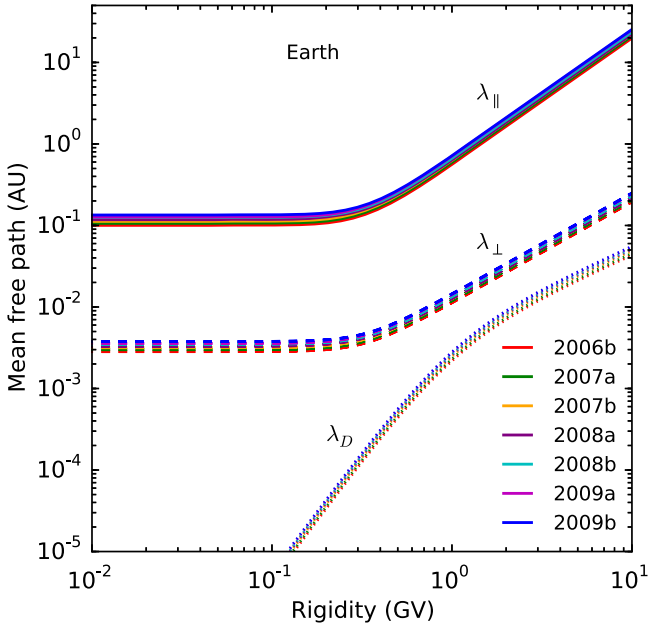

Figure 7. Assumed rigidity dependence of the main diffusion coefficients and the drift coefficient at the Earth. Here, the corresponding parallel ($\lambda_\parallel$) and perpendicular mean free paths ($\lambda_\perp \equiv \lambda_{\perp r} \equiv \lambda_{\perp\theta}$) and the drift scale ($\lambda_D$), all in AU, are depicted with colored lines, indicative of the changes needed to reproduce the observations from 2006b (lower lines, beginning with red curves) to 2009b (upper lines, ending with blue curves).

energy so that the modulation process becomes diffusion-dominated.

Figure 5(b) is similar to Figure 5(a) except that the computed spectra are now shown over a wider energy range, down to 10 MeV, with respect to the very LIS to illustrate the total modulation of electrons as computed with this modeling approach, over this special solar minimum modulation period.

The flux ratios are shown again in Figure 6 now in comparison with the corresponding computed ratios based on the spectra shown in Figures 5(a), (b). Care was taken to reproduce the 2006b spectrum from the lowest to the highest energy values, then we attempted to do the same for every following semester using the trends in the HCS and HMF values as shown in Figures 4(a), (b) and the subsequent diffusion and drift coefficients as described above. Clearly, we were able to accomplish this for all the observed spectra with $E \geqslant \sim$200 MeV. Below this, energy deviations are found between the modeled spectra and the observational spectra, which may be expected since the fluxes for the lowest electron energies could not be determined with the same accuracy as the previous semesters. However, the overall trends are well reproduced by this modeling approach. This figure highlights how the CR electron spectra had increased with respect to the second semester of 2006. It follows that at 1 GeV, the electron differential intensity increased over this 3.5 year period by a factor of $\sim$1.5, whereas at 100 MeV it increased by a factor of $\sim$3.5. This is less than what was found for protons over the same period (Potgieter et al. 2014).

The changes to the modulation parameters as required for this process are summarized in Table 1. These changes, and in particular, the assumed rigidity dependence of the three diffusion coefficients and the drift coefficient at the Earth, are illustrated in Figure 7. Using the general relationship between the mean free path and the corresponding diffusion or drift coefficients, $\lambda = 3K/\nu$, the parallel and perpendicular mean free paths, as well as the drift scale, all in AU, are plotted together in Figure 7, where v is the electrons' speed. Since the rigidity dependence of $\lambda_{\perp\theta}$ is identical to that of $\lambda_{\perp r}$, it is not shown separately. Clearly, these relatively small adjustments in the modulation parameters with time, in addition to the changes in the tilt angles and HMF magnitude, are adequate to reproduce the observed electron spectra. This also serves to illustrate the relative sensitivity of the model to these basic modulation parameters.

The modulation trend (recovery in intensity from 2006b to minimum modulation in 2009a, 2009b) is further illustrated in Figure 8 for 1.0 GeV electrons, comparing the observations with the corresponding computed spectra. It follows that the clear increasing trend (recovery) in the electron intensity from 2006b to 2007b was interrupted when solar activity increased for a few months in 2008 instead of keeping up the recovering trend as before this period. This is evident in how α increased during this period, as shown in Figure 4(a), with even the NM count rate leveling off during 2008. However, the recovery then resumed at a faster rate from mid-2008 to mid-2009. The agreement between the model and the observations is quite good, except for the second semester of 2009 (2009b) when the model predicts a slower increasing trend (recovery) in the intensity based on the modulation parameters used as input, while the observations indicate a flattening.

6. DISCUSSION

The aim of the study was to reproduce a selection of seven six-month averaged electron spectra as observed by the *PAMELA* space experiment. This was done by using averaged values for α and B as the magnitude of the HMF as input in the numerical model as indicated in the two first rows of Table 1 and shown in Figures 4(a) and (b). These two modulation parameters are considered the most important time-dependent

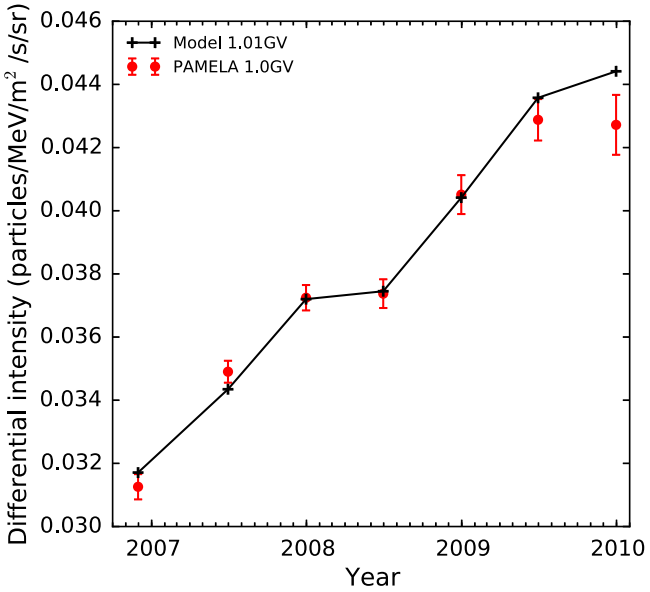

Figure 8. Observed intensity increase (red data points with error bars) for 1 GeV electrons from the second semester of 2006 to the second semester of 2009 in comparison with the corresponding computed values for the same period (black line).

ones because they are both very good proxies for solar activity when it comes to the modulation of charged particles. Based on our assumptions, changing B also feeds directly into expressions for the diffusion coefficients and the drift coefficient, as in Equations (9)–(13). However, in order to reasonably reproduce the seven observed spectra, the overall value of the diffusion coefficients had to be increased moderately for every semester in addition to the changes brought about by changing the values of α and B. This is illustrated in Table 1 by the increasing value of $\lambda_{\parallel}$, and subsequently also $\lambda_{\perp r}$, from 2006b to 2009b, for example, by a factor of 1.33 at 100 MeV. The overall rigidity dependence of the coefficients had to be changed very little as shown in Figure 7.

The specific form of this rigidity (energy) dependence is, however, very important. Based on turbulence theory, predictions have been made over the years about the rigidity dependence of the diffusion coefficients at the Earth. It was found that for electrons, in contrast to protons, for example, this coefficient is essentially independent of $E < \sim$0.5 GeV, with a possible increase at $E < \sim$20 MeV, depending on what particular theoretical turbulence assumptions are followed; see, e.g., Bieber et al. (1994), Potgieter (1996, 2000), Burger et al. (2000), and Teufel & Schlickeiser (2002). We confirm this basic prediction as the outcome of comparing the *PAMELA* electron spectra with our comprehensive model. This was also found in a comparison between a similar model and the electron observations made by *Voyager 1* in the outer heliosphere (Potgieter & Nndanganeni 2013b).

Adjusting the ratio between the parallel and the two perpendicular diffusion coefficients, as a function of energy, as required by turbulence theory (see e.g., Burger et al. 2000), was found to be relatively unimportant as long as it is done only at higher energies as illustrated in Figure 7. However, at $E < 300$ MeV the ratio between these diffusion coefficients is very important and is found to remain unchanged. A small enhancement of the polar dependence of perpendicular diffusion in the polar direction is still required given that the HMF also had to be modified in the polar regions of the heliosphere.

Concerning drifts, the "weak scattering approach" at low energies as given in Equation (12) is too simple and the modification as given by Equation (13) is required even under perfect solar minimum conditions as in 2009. We confirm the required modification effects of turbulence on particle drifts at lower energies (see also Ngobeni & Potgieter 2015).

A very important issue and result of doing this detailed study is the long-standing issue of what the total modulation is for Galactic electrons in the heliosphere, that is, between the HP and the Earth. This question can now be answered with confidence because of the *Voyager 1* measurements of the position of the HP and the very LIS. These values had to be cleverly handled before. Based on the spectra shown in Figure 5(b), we calculate the modulation factor (MF) as the ratio of the intensity of the LIS at the HP to the intensity at the Earth in terms of kinetic energy for the periods 2009a and 2009b, that is, for ideal solar minimum conditions. This is given in Table 2. Clearly, the total MF is rather small at high energies but quite significant at low energies. A very interesting aspect for electron modulation is that with $E < \sim$50 MeV this MF will remain the same as long as the rigidity dependence of the diffusion coefficients is kept constant at these low energies as shown in Figure 7 (see also Potgieter 1996). This is not at all the case for protons and CR nuclei which experience much larger adiabatic energy losses toward the inner heliosphere so that their modulated spectral shapes are determined by these adiabatic energy losses not the rigidity dependence of the diffusion coefficients.

The next phase of this study is to apply this model to the positron spectra observed by *PAMELA* for the same period. Together with studying electron spectra at the same rigidity as protons, a comprehensive study can be performed about how particle drifts affect modulation under very quiet solar activity conditions. This should clarify the role that drifts play during periods of unusual low solar activity.

7. SUMMARY AND CONCLUSIONS

PAMELA electron spectra between 80 MeV and 30 GeV as observed from mid-2006 to the end of 2009 (Adriani et al. 2015) were used in a comparative study with a comprehensive 3D numerical modulation model including particle drifts and an inner heliosheath that changes its width with the solar cycle. A new very LIS for electrons has been applied as constructed from electron observations from *Voyager 1* and *PAMELA* (see also Potgieter 2014b). Together with the observed position of the HP, the total modulation between the HP and the Earth could be computed with improved confidence. It was found that at 100 MeV the electron intensity decreases over a distance of 121 AU by a factor of 530.

The main features of the observed electron spectra, for example the softening of the spectra from 2006 to the end of 2009, could be reproduced by this modeling approach, which was also followed for protons (Potgieter et al. 2014). It is found that the 2009 solar minimum period was indeed different than previous solar minimum modulation periods and appears to be diffusion-dominated because of the very low solar activity observed. However, although the role of particle drifts was less obvious, it is confirmed here that this study serves to illustrate the importance of each of the modulation processes, including drifts. Similar to our proton study (Potgieter et al. 2014), it is

Table 2
The Modulation Factor (MF) as the Ratio of the Very LIS Intensity to the Computed Intensity at the Earth in Terms of Kinetic Energy E in GeV for the Periods 2009a (MFa) and 2009b (MFb)

E (GeV)	0.05	0.10	0.20	0.50	0.80	1.0	3.0	5.0	8.0	10.0
MFa	1030	530	140	17.9	7.30	5.14	1.76	1.38	1.21	1.16
MFb	759	438	128	17.3	7.21	5.08	1.75	1.38	1.21	1.16

concluded that all modulation processes contributed to the observed changes in the observed spectra.

From a theoretical point of view, it is confirmed that for electrons the rigidity dependence of the three basic diffusion coefficients is essentially independent of E below $\sim$0.5 GeV. Adjusting the small ratio between the parallel and the two perpendicular diffusion coefficients as a function of energy (rigidity) was found to be relatively unimportant as long it is restricted to higher energies. Concerning drifts, the weak scattering approach at low energies is found to be too simple and a modification is required even under perfect solar minimum conditions as in 2009.

The main features evident from the observed spectra from 2006b to 2009b are reproduced in detail by this modeling approach: (1) the spectra exhibit maximum values between $\sim$500 and $\sim$800 MeV and these maxima shift gradually to lower energies during this period (this occurs because of the changing interplay between drifts and diffusion) and (2) at around 100 MeV, the spectra show minima which shift gradually to higher energies as drifts phase out with decreasing energy so that the modulation process becomes diffusion-dominated. This type of minimum in electron spectra does not occur for proton spectra.

The South African authors express their gratitude for the partial funding by the South African National Research Foundation (NRF) under the Italy–South African Research Cooperation Programme, and under the Incentive and Competitive Grants for Rated Researchers. They also thank the INFN in Italy for the partial financial support when visiting in Trieste, and in Rome, over a span of a few years. E. E. V. thanks the NRF and the South African Space Agency (SANSA) for partial financial support during his PhD study.

REFERENCES

Adriani, O., Barbarino, G. C., Bazilevskaya, G. A., et al. 2011, PhRvL, 106, 201101
Adriani, O., Barbarino, G. C., Bazilevskaya, G. A., et al. 2013, ApJ, 765, 91
Adriani, O., Barbarino, G. C., Bazilevskaya, G. A., et al. 2015, ApJ, 810, 142
Bieber, J. W., Matthaeus, W. H., Smith, C. W., et al. 1994, ApJ, 420, 294
Boezio, M., Pierce, M., Picozza, P., et al. 2009, NJPh, 11, 105023
Burger, R. A., Potgieter, M. S., & Heber, B. 2000, JGR, 105, 27447
Cliver, E. W., Richardson, I. G., & Ling, A. G. 2011, SSRv, 176, 3
de Simone, N., di Felice, V., Giesler, J., et al. 2011, ASTRA, 7, 425
Di Felice, V. 2010, PhD thesis, Univ. Rome Tor Vergata
Effenberger, F., Fichtner, H., Scherer, K., et al. 2012, ApJ, 750, 108
Ferreira, S. E. S. 2005, AdSpR, 35, 586
Ferreira, S. E. S., Potgieter, M. S., Moeketsi, D. M., Heber, B., & Fichtner, H. 2003, ApJ, 594, 552
Gurnett, D. A., Kurth, W. S., Burlaga, L. F., & Ness, N. F. 2013, Sci, 341, 1489
Heber, B., & Potgieter, M. S. 2006, SSRv, 127, 117
Hoeksema, J. T. 1991, AdSpR, 11, 15
Kóta, J. 2013, SSRv, 176, 391
Menn, W., Adriani, O., Barbarino, G. C., et al. 2013, AdSpR, 51, 209
Mocchiutti, E., Adriani, O., Barbarino, G. C., et al. 2011, NIMPA, 630, 28
Moeketsi, D. M., Potgieter, M. S., Ferreira, S. E. S., et al. 2005, AdSpR, 35, 597
Munini, R., Di Felice, V., Adriani, O., et al. 2013, Proc. 33rd ICRC, 0377
Ngobeni, M. D., & Potgieter, M. S. 2011, AdSpR, 48, 300
Ngobeni, M. D., & Potgieter, M. S. 2015, AdSpR, 56, 1525
Nkosi, G. S., Potgieter, M. S., & Webber, W. R. 2011, AdSpR, 48, 1480
Parker, E. N. 1965, P&SS, 13, 9
Potgieter, M. S. 1996, JGR, 101, 24411
Potgieter, M. S. 2000, JGR, 105, 18295
Potgieter, M. S. 2013, LRSP, 10, 3
Potgieter, M. S. 2014a, AdSpR, 53, 1415
Potgieter, M. S. 2014b, BrJPh, 44, 581
Potgieter, M. S., & Nndanganeni, R. R. 2013a, APh, 48, 25
Potgieter, M. S., & Nndanganeni, R. R. 2013b, Ap&SS, 345, 33
Potgieter, M. S., Vos, E. E., Boezio, M., et al. 2014, SoPh, 289, 391
Raath, J. L., Potgieter, M. S., Strauss, R. D., & Kopp, A. 2015, SoPh, submitted
Scherer, K., Fichtner, H., Strauss, R. D., et al. 2011, ApJ, 735, 128
Shalchi, A. 2009, Astrophysics and Space Science Library, Vol. 362 (Berlin: Springer)
Smith, C. W., & Bieber, J. W. 1991, ApJ, 370, 435
Stone, E. C., Cummings, A. C., McDonald, F. B., et al. 2013, Sci, 341, 150
Strauss, R. T., & Potgieter, M. S. 2014a, SoPh, 289, 3197
Strauss, R. T., & Potgieter, M. S. 2014b, AdSpR, 53, 1015
Strauss, R. T., Potgieter, M. S., Kopp, A., & Büshing, I. 2011, JGR, 116, A12105
Strauss, R. T., Potgieter, M. S., Ferreira, S. E. S., Fichtner, H., Scherer, K., et al. 2013, ApJL, 765, L18
Strong, A. W., Orlando, E., & Jaffe, T. R. 2011, A&A, 534, A54
Teufel, A., & Schlickeiser, R. 2002, A&A, 393, 703
Vos, E. E., Potgieter, M. S., Boezio, M., et al. 2013, Proc. 33rd ICRC, 0276